



Selective removal of ATP degradation products from food matrices II: Rapid screening of hypoxanthine and inosine by molecularly imprinted matrix solid-phase dispersion for evaluation of fish freshness



M.C. Cela-Pérez^a, L. Barbosa-Pereira^b, X. Vecino^b, M. Pérez-Ameneiro^b,
Aurora Lasagabaster Latorre^{a,c}, J.M. López-Vilariño^a, M.V. González Rodríguez^{a,*},
A.B. Moldes^b, J.M. Cruz^b

^a Grupo de Polímeros, Centro de Investigaciones Tecnológicas (CIT), Departamento de Física, Escuela Universitaria Politécnica, Universidad de A Coruña (UDC), Campus de Ferrol, 15471 Ferrol, Spain

^b Departamento de Ingeniería Química, Escuela de Ingeniería Industrial (EII), Universidad de Vigo, Campus As Lagoas, Marcosende 36310, Vigo-Pontevedra, Spain

^c Departamento de Química Orgánica I, Facultad de Óptica y Optometría, Universidad Complutense de Madrid, Arcos de Jalón no. 118, Madrid 28037, Spain

ARTICLE INFO

Article history:

Received 19 September 2014

Received in revised form

19 December 2014

Accepted 23 December 2014

Available online 3 January 2015

Keywords:

Molecularly imprinted polymer

Matrix solid-phase dispersion

Freshness

Fish samples

Hypoxanthine

Inosine

ABSTRACT

A water compatible molecularly imprinted polymer (MIP), synthesized using theophylline (TPH) as dummy-template and acrylamide (AM) as functional monomer, has been employed as supporting material in matrix solid-phase dispersion combined with ultra performance liquid chromatography–photodiode array detection (MSPD–UPLC–PDA) for selective determination of adenosine triphosphate (ATP) derivatives in fish samples. ATP degradation products are used as freshness index for assessment of fish quality. The solid sample was directly blended with MIP in MSPD procedure resulting in sample disruption and subsequent adsorption of the compounds on the MIP. By using *n*-hexane and ammonium hydroxide aqueous solution at pH 9 as the washing and elution solvent, respectively, satisfactory recoveries and clean chromatograms have been obtained. Good linearity for hypoxanthine (HYP) and inosine (INO) has been observed with correlation coefficients (R^2) of 0.9987 and 0.9986, respectively. The recoveries of the two ATP derivatives at three different spiked levels ranged from 106.5% to 113.4% for HYP and from 103.1% to 111.2% for INO, with average relative standard deviations lower than 4.2% in both cases. This new method, which is rapid, simple and sensitive, can be used as an alternative tool to conventional tedious methods.

© 2014 Elsevier B.V. All rights reserved.

1. Introduction

A large number of post-mortem reactions are initiated in fish (glycolysis, proteolysis and lipolysis) immediately after the animal is slaughtered, affecting its quality and freshness conditions. One of the most important changes consists of the formation of nucleotide and nucleoside metabolites resulting from ATP degradation [1]. ATP degradation to ADP (adenosine diphosphate) and AMP (adenosine monophosphate) takes place rapidly, with the subsequent accumulation of IMP (inosine 5'-monophosphate) [2].

The IMP is hydrolyzed by autolytic enzymes (5'-nucleotidase) to inosine (INO), which, in turn, is degraded to hypoxanthine (HYP) by autolytic and/or microbial action (nucleoside phosphorylase) [3,4]. Next, HYP will be oxidized to xanthine (XAN) and then to uric acid (UA) through a much slower reaction, due to xanthine oxidase (XO) in case of spoilage by microorganisms [5–7].

The pathway of ATP catabolism as a degradative sequence has been widely studied in different fish species [7–12] besides beef [13,14], chicken [15,16] or pork meat [2,3,17–19] and some of the above mentioned nucleotide metabolites have been proposed as freshness indexes in quality assessment [18,19]. Several analytical methods such as electrophoresis [20,21], radioimmunoassay [22], nuclear magnetic resonance spectroscopy (NMR) [23] or amperometric and voltamperometric methods [24] have been reported for quantitative determination of these compounds. Besides, in recent

* Corresponding author.

Tel.: +34 981 337 400 (3051/3485); fax: +34 981 337 416.

E-mail address: victoria.gonzalez.rodriguez@udc.es (M.V. González Rodríguez).

years, the use of biosensors has been introduced as an alternative [15]. In particular, a significant number of biosensors have been designed based on the enzymatic reaction catalyzed by the XO [25,26]. However these XO based biosensors have some common drawbacks such as poor stability, non-reusability, slow electron transfer and complexity of immobilization. Conversely, versatility, short analytical time and high resolution have made high performance liquid chromatography (HPLC) the most widely used technique for the analysis of nucleotides and nucleosides in biological samples [7,27,28].

Prior to HPLC determination, a sample preparation process is needed which is really the critical step of the whole analytical process. It should remove potential interferences, pre-concentrate analytes and sometimes, convert them into a suitable form for determination or separation. More to the point, it must provide a robust and reproducible method, independent of variations in the matrix sample. Nowadays, it is also very important to reduce the initial sample size, improve the selectivity of the extraction process, minimize the use of organic solvents and facilitate the automation of the procedure [29]. Solid-phase extraction (SPE) is probably the most widely used technique of sample preparation today, but sample matrix interferences co-elute with the analytes of interest due to the lack of selectivity of common sorbents used; hence, subsequent clean-up steps are required. The use of molecularly imprinted polymers (MIPs) as selective sorbent materials in SPE (MISPE) avoids this problem. MIPs allow analyte pre-concentration and elimination of sample interferences [29,30] in a single step, since they are synthetic materials with artificially generated recognition sites able to rebind a target molecule specifically, even in preference to other closely-related compounds [31,32].

As a general rule for tissue samples, an exhaustive treatment is always required before SPE. The tissue is usually homogenized and centrifuged and only the extract is passed through the MISPE cartridge. However, cell disruption is often incomplete. By contrast, molecularly imprinted matrix solid-phase dispersion (MIP-MSPD) performs simultaneous disruption, extraction and clean-up of solid, semi-solid and highly viscous samples [33–36]. Furthermore, the complete sample disruption and dispersal onto MIP particles occurs, providing an enhanced surface area for subsequent extraction step. MIP-MSPD is less time consuming and manual-intensive as well as more eco-compatible than MISPE. Experimentally, the sample is placed in a glass mortar and blended with the sorbent until complete disruption and dispersion of the sample on the solid support is attained. Then, the mixture is directly packed into an empty cartridge and analytes are eluted after a proper washing step to remove interfering compounds.

This work represents the first attempt to use MIPs as MSPD sorbent to develop a new MIP-MSPD-UPLC-PDA method for the selective extraction and determination of ATP related compounds in fish samples. Besides, it is well known that IMP contributes to the pleasant flavor of fresh fish and its degradation to INO and then to HYP is responsible for the progressive loss of the desirable flavor and the development of the stinking fishy smell [37,38]. In addition, it is accepted that HYP is accumulated owing to INO rapid degradation to HYP and its subsequent slow transformation into XAN and UA by xanthine oxidase [17,18]. Thus, HYP has been chosen to determine the freshness of fish.

2. Experimental

2.1. Material

Theophylline (TPH), INO, XAN, UA and trifluoroacetic acid (TFA) were obtained from Sigma-Aldrich (Steinheim, Germany). Acrylamide (AM), ethylene glycol dimethacrylate (EGDMA), 2,

2-azobisisobutyronitrile (AIBN) and ammonium hydroxide solution (25% in water) were supplied from Fluka (Buchs, Switzerland). Ethanol (EtOH), methanol (MeOH) and hexane were obtained from Merck (Darmstadt, Germany), chloroform (CHCl₃) was from Scharlab (Barcelona, Spain) and acetic acid glacial (AcOH) from Panreac (Barcelona, Spain). HYP was purchased from ACROS organics (Geel, Belgium). Water used in the experiments was purified using a Milli Q Ultrapure water-purification system (Millipore, Bedford, MA, USA).

2.2. UPLC-PDA analysis

UPLC analyses were performed using an Acquity system from Waters (Milford, MA, USA) with gradient pump and automatic injector. Chromatographic experiments were carried out using a stainless steel column Acquity UPLC™ BEH C₁₈, 2.1 × 50 mm, 1.7 μm (apt to work in a 1–12 pH range, at temperatures between 20 and 90 °C, and capable of operating at pressures up to 15,000 psi). Detection was carried out using a photodiode array detector (PDA) set in the range of 200–400 nm. Output signals were monitored and integrated using a personal computer operated under the Empower 2 software (Waters). Wavelength of 250 nm for HYP analysis was selected as output PDA signals. A two solvent gradient elution was performed, with flow rate of 0.5 mL min⁻¹ and injection volume of 3 μL. The mobile phase consisted of aqueous TFA (A) (0.1% TFA in deionized water, pH 2.2, v/v) and MeOH (B) gradient [39]. The gradient elution profile starts at 99% of A, was linearly increased to 70% of A in 0.70 min and then brought back to the initial conditions at 1 min.

2.3. Preparation of the molecularly imprinted polymer

The MIP having HYP recognition sites was prepared according to a previous work performed by our research group by non-covalent precipitation polymerization. The MIP has already been fully characterized [40]. TPH as dummy-template molecule (1 mmol) was dissolved in 60 mL of chloroform and subsequently, 4 mmol of AM as functional monomer was mixed until homogenization. Next, 20 mmol of EGDMA as cross-linker monomer was added to the mixture, followed by 0.5 mmol of the initiator of the polymerization, AIBN.

The pre-polymerization mixture was degassed in a sonicating bath and purged with nitrogen for 5 min. Polymerization took place in a water bath at 60 °C for 24 h. The final polymer was dried at 40 °C. TPH was removed by Soxhlet extraction with MeOH for 48 h. The complete removal of TPH from the MIP was assessed via UPLC-PDA method. A non-imprinted polymer (NIP) was similarly prepared excluding TPH from the pre-polymerization media.

2.4. Binding evaluation of TPH-AM-EDMA-MIP

Batch binding assays were carried out for evaluation of the MIPs molecular recognition behavior. Taking into account the fact that these MIPs will be used to extract HYP from fish samples, the solvent for batch rebinding assays was selected according to community legislation [41], which establishes water:EtOH (9:1) as simulant for fresh, cooled, processed salted or smoked fish.

Pre-weighed amounts (0.2 g) of cleaned MIPs were placed into glasses for 5 min incubation in ultrasonic bath at room temperature with eight water:EtOH (9:1) solutions (4 mL) of HYP (from 5.25 to 1009 μg mL⁻¹). After incubation, supernatants were removed by filtration and analyzed by UPLC-PDA at 250 nm to determine HYP residual concentrations, *C* (μmol L⁻¹). HYP adsorbed concentrations, *q* (μmol g⁻¹ or μg g⁻¹), were calculated by subtracting *C* from the initial concentrations of HYP. Batch binding experiments were done in a similar way with blank polymers.

The specificity of the polymer was then estimated by the imprinting factor (*IF*) $IF = K_{pMIP}/K_{pNIP}$, where K_{pMIP} is the partition coefficient of a compound on the imprinted polymer and K_{pNIP} is the partition coefficient of the same compound on the non-imprinted polymer. The partition coefficient is defined as the ratio of the amount of HYP bound to the polymer (q , $\mu\text{mol g}^{-1}$) relative to the concentration of free HYP (C , $\mu\text{mol L}^{-1}$). This normalization method removes binding due to non-specific interactions [42,43].

To further investigate the imprinting effect and determine the binding properties (adsorption capacity, binding constants etc.) several binding models such as the discrete Langmuir and bi-Langmuir models and the continuous Freundlich isotherm model (FI), were applied to fit the equilibrium data. The model with the highest degree of correlation was finally chosen [43,44].

2.4.1. Swelling

To further explain rebinding behavior MIP and NIP swelling was conducted in the binding solvent water:EtOH (9:1) for comparison with results in ACN:water 4:1 (v:v) and CHCl_3 , performed in a previous work [40]. The experimental procedure is similar to that described by Sellergren and Shea [45]. Dry polymer ($\cong 0.20$ – 0.30 mL) was placed in a 1 mL graduated test tube. Excess solvent was then added to the tube and the polymer sonicated in order to remove air bubbles. The tube was closed and left to stand for 24 h at room temperature. Excess solvent was then removed and final volumes were recorded. The swelling ratio was given as volume of the swollen polymer to volume of dry polymer. The average values of triplicate independent results were obtained.

2.5. Selectivity evaluation of TPH-AM-EDMA-MIP

Additional batch binding assays were performed to test selectivity of the MIP towards other ATP degradation products such as INO, XAN and UA. Individual solutions of INO (from 5.000 to 1000 $\mu\text{g mL}^{-1}$), XAN and UA (from 5.000 to 400.0 $\mu\text{g mL}^{-1}$) in water:EtOH (9:1) were employed for individual selectivity analysis and mixture solutions (from 5.000 to 400.0 $\mu\text{g mL}^{-1}$) were used in competitive assays for cross-selectivity evaluation. These concentration ranges have been selected according to solubility properties. The above mentioned binding isotherm models were also applied to determine the selectivity properties. The specific selectivity factor (*SF*) was calculated taking the ratio of imprinting factors, $SF = IF_1/IF_2$ where IF_1 and IF_2 are the imprinting factors for two different substrates [42–44].

2.6. MSPD procedure

The schematic procedure of the MIP-MSPD-UPLC-PDA is shown in Fig. 1. An aliquot of 0.2 g of fish meat and 0.4 g of MIP sorbent (1:2) were placed in a small porcelain mortar and blended together until a homogeneous mixture was obtained. Then, the mixture was loaded into a SPE cartridge (6 mL pre-fritted, 20 μm porosity, polypropylene tubes) which was pre-packed with 0.05 g of cleaned MIP and the column was connected to a VisiprepTM-DL Solid Phase Extraction Vacuum Manifolds, equipped with integral flow control valves and disposable Teflon[®] flow control valve liners (SUPELCO, Bellefonte, PA, USA). The cartridge was rinsed with 2 mL of hexane, the eluent was evaporated to dryness under vacuum at room temperature and the residues were re-dissolved in 2 mL of Milli Q water for further UPLC-PDA analysis. Subsequently, the cartridge was eluted with 4 mL of ammonium hydroxide solution (5.55×10^{-6} M, pH 9) and the basic eluent was directly carried to UPLC-PDA for HYP determination.

3. Results and discussion

3.1. Recognition properties of the TPH-AM-EDMA-MIP

Fig. 2(a) compares the adsorption isotherm of HYP on MIP and NIP. Batch concentrations and binding amounts have been plotted as the abscissa and ordinate, respectively. A different behavior is observed for MIP and NIP. While the amount of HYP bound to the MIP at equilibrium rinsed gradually with concentration, a saturation level was reached for NIP at the fourth concentration assayed. The MIP capacity for the template concentration range studied in this work (up to 1000 $\mu\text{g mL}^{-1}$), was nearly 3500 $\mu\text{g g}^{-1}$, which is in the range of other MIPs prepared by non-covalent imprinting [46,47], whereas the corresponding NIP value lied below 1500 $\mu\text{g g}^{-1}$. These data suggest a molecular imprinting effect [48].

The *IF* values > 1 confirmed the conclusion explained in the preceding paragraph. The average *IF* (\bar{IF}) was 2.25, although some variability was observed throughout the concentration range; the maximum value of 6.82 was found for the first concentration tested ($5.246 \mu\text{g mL}^{-1}$).

The equilibrium data fitted well the FI model as evidenced by the relatively good fit to linear regression analysis ($R^2 \geq 0.9$) (Table 1). Fig. 2(b) depicts the FI in $\log K$ - $\log N$ format. The most visible difference between MIP and NIP is the higher capacity of the former within the measured concentration window. This can be seen in the higher positioning of the MIP line. This qualitative assessment was confirmed by the parameters calculated from the FI model which are summarized in Table 1. The MIP binding capacity value (N_{K1-K8}) was 368.3 $\mu\text{g g}^{-1}$ or 2.706 $\mu\text{mol g}^{-1}$ which was about 100-fold the corresponding N_{NIP} value (3.811 $\mu\text{g g}^{-1}$ or 0.028 $\mu\text{mol g}^{-1}$). Furthermore, the average affinity of binding sites (\bar{K}_{K1-K8}) for the MIP ($7.95 \times 10^2 \text{ M}^{-1}$) was 2.5 times higher than the NIP value ($3.16 \times 10^2 \text{ M}^{-1}$).

The range of binding affinity was constrained within the limits of the analytical window (K_{min} - K_{max}) in Fig. 2(c). The graph shows the relationship between the fraction of binding sites (N , $\mu\text{mol g}^{-1}$) and the affinity constants in log format ($\log K$, M^{-1}). The control polymer had very few binding sites distributed throughout the entire affinity range compared with MIP, although the latter had numerous low affinity binding sites and a few high affinity binding sites.

In fact, reasonably good binding parameter values have been achieved for HYP on the MIP in aqueous solvent. Nonetheless, these values are lower than those obtained in ACN:water (4:1 v/v) [40], owing to the fact that the rebinding to MIPs is strongly dependent on the solvent. The solvent can affect rebinding in two ways. First of all, molecular recognition with the MIP in solvents of low to medium polarity is mainly driven by H-bonding [49]. When increasing the aqueous content in the rebinding solvent, polar templates such as HYP are less retained on MIPs due to the enthalpy driven hydrophobic effect.

Secondly, a solvent induced swelling/shrinking process can affect the shape of the cavity and the distance between functional groups and due to this, MIP can lose its specificity when exposed to the “wrong conditions” [50]. MIP and NIP swell in water:EtOH (9:1) but to a lesser extent than in ACN:water (4:1 v/v) and the porogen, CHCl_3 (MIP swelling ratios are: 2.2 ± 0.1 , 4.2 ± 0.7 and 7.9 ± 0.1 and NIP swelling ratios are: 2.8 ± 0.1 , 5.1 ± 0.1 and 8.4 ± 0.8 in water:EtOH (9:1), ACN:water (4:1 v/v) and CHCl_3 , respectively) [40].

Anyway, the observed relatively good behavior of the MIP for HYP in aqueous media is mainly attributed to the following two reasons: (1) the addition of a certain amount of organic solvent (10% ethanol) into the pure aqueous solutions of the template and (2) the election of a highly polar functional monomer such as AM, instead of the more usual MAA, which increases the MIP's surface hydrophilicity. AM is more soluble in water, 2150 g L^{-1} compared to 89 g L^{-1} for acrylic acid, and forms stronger hydrogen-bonds in

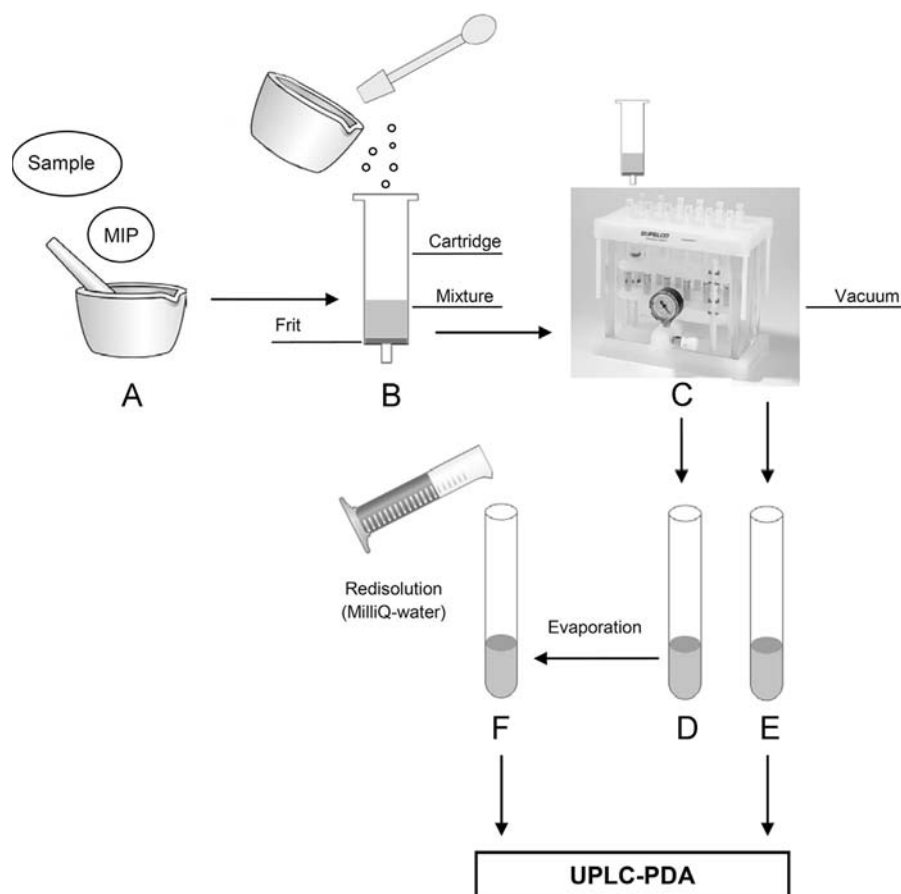


Fig. 1. Schematic procedure of MIP-MSPD: (A) sample-MIP sorbent blending, (B) transfer blend to cartridge, (C) washing and elution under vacuum, (D) washing eluate (hexane) to be evaporated, (E) redissolution of D in Milli-Q water and (F) basic extraction eluate containing the ATP derivatives.

polar protic solvents than acrylic acid. Both strategies reduce the hydrophobically driven nonspecific bindings of the MIP, thus leading to its water compatibility despite the lower swelling compared to porogen [51–53]

3.2. Selectivity properties

3.2.1. Individual selectivity properties

To measure the selective recognition of HYP, the separate binding of competitive compounds was performed in the first place. Fig. 3 (a) exhibits the FI isotherms in log format for visual comparison of the binding capabilities of INO, XAN and UA. The log K –log N FI isotherm obtained for HYP was overlaid for comparison. Strikingly, the highest position in the graph was occupied by the bulky INO molecule, followed by HYP and XAN, which crossed each other, which are in turn over UA. Furthermore, the most important binding parameters determined by the FI model are compiled in Table 2. The data confirm the greater binding capacity (N_{K1-K8}) for INO ($508.8 \mu\text{g g}^{-1}$ or $1.897 \mu\text{mol g}^{-1}$) and HYP ($368.3 \mu\text{g g}^{-1}$ or $2.706 \mu\text{mol g}^{-1}$) (Table 1) in relation to XAN ($119.9 \mu\text{g g}^{-1}$ or $0.788 \mu\text{mol g}^{-1}$) and UA ($89.26 \mu\text{g g}^{-1}$ or $0.531 \mu\text{mol g}^{-1}$). According to the FI model, the average affinity of binding sites (\overline{K}_{K1-K8}) for INO was about 4-fold higher in the MIP ($2.50 \times 10^3 \text{ M}^{-1}$) than in the NIP ($6.18 \times 10^2 \text{ M}^{-1}$) and thrice the value calculated for HYP ($7.95 \times 10^2 \text{ M}^{-1}$).

Moreover, a high similar average IF has been achieved for INO, $\overline{IF}=2.20$, compared to and HYP ($\overline{IF}=2.25$); again the highest $IF_{\text{max}}=9.51$ was obtained for the lowest INO concentration tested. Hence, it can be concluded that the MIP are appropriate to determine INO in addition to HYP, within the range of concentrations studied.

Regarding XAN, the corresponding affinity constant value ($\overline{K}_{K1-K6}=2.47 \times 10^3 \text{ M}^{-1}$) was higher than the value calculated for HYP, although the number of binding sites decreased 3-fold. Moreover, the average imprinting factor ($\overline{IF}=1.85$) is $\cong 1.5$ -fold lower than HYP. The highest IF values for XAN are also encountered at the lowest concentration assayed ($IF_{\text{max}}=6.13$), although the IF was below 1 for higher amounts of XAN, indicating unspecific adsorption. These data reveal that the MIP could also be used to determine XAN in fish samples, provided that the amount of XAN in the sample is $\leq 5 \mu\text{g mL}^{-1}$. On the contrary, the results obtained for UA show a MIP binding capacity and affinity constant quite lower than the NIP values. In coherence with this, the corresponding imprinting factors are the smallest and close to unity ($\overline{IF}=1.10$). Furthermore, no adsorption of UA was observed at the lowest concentration tested ($400.0 \mu\text{g mL}^{-1}$). Thus, the MIP is less suitable to determine the last ATP derivative in aqueous media.

From another point of view, the average selectivity factors (\overline{SF}) for HYP in relation to INO, XAN and UA were 0.969, 1.45 and 2.99 respectively. These \overline{SF} values were calculated considering the \overline{IF} of the three lowest concentration studied for HYP and INO to avoid false interpretations of relative selectivity (since the assays were carried out for HYP and INO from 5.000 to 1000 $\mu\text{g mL}^{-1}$ and for XAN and UA from 5.000 to 400.0 $\mu\text{g mL}^{-1}$). Furthermore, SF_{max} at the lowest concentration assayed ($\cong 5 \mu\text{g mL}^{-1}$) were 0.717 (INO), 1.11 (XAN) and 6.40 (UA). These results corroborate the highest selectivity of the MIP for INO followed by HYP, XAN and UA in agreement with the conclusions extracted from Fig. 3(a) and Tables 1 and 2.

In summary, both swelling and selectivity studies suggest that shape selectivity is not the dominant mechanism for molecular recognition. First of all, among the different ATP derivatives

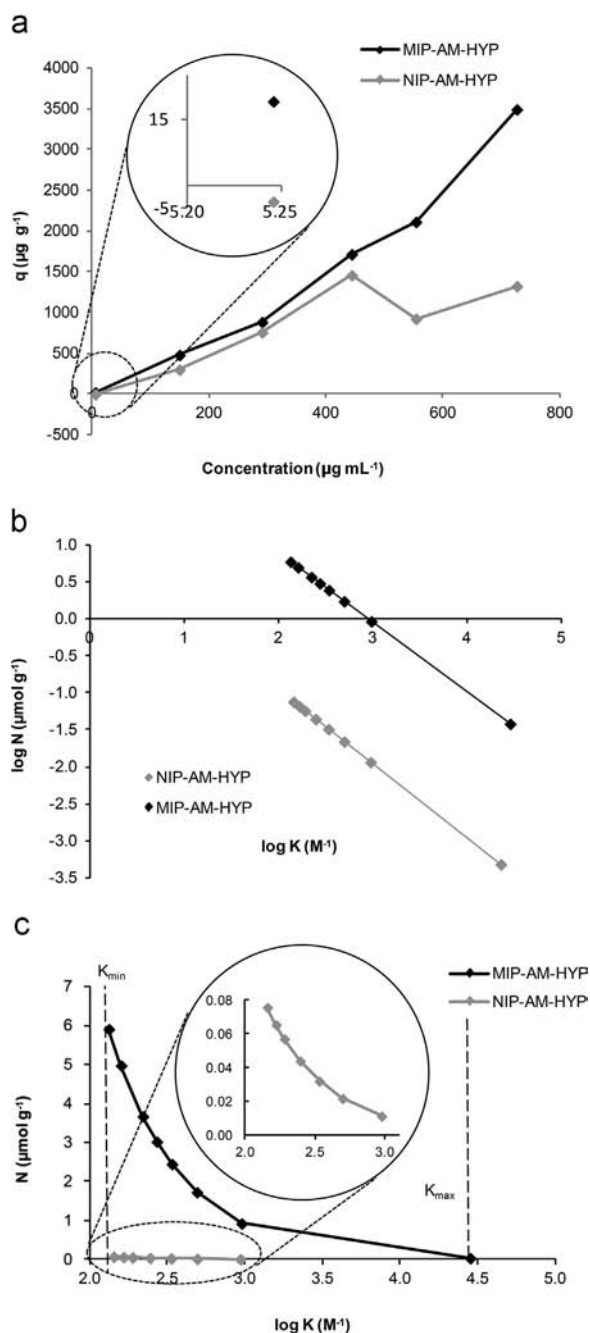


Fig. 2. (a) Adsorption isotherm of HYP on MIP and NIP in the range 5.246–726.3 $\mu\text{g mL}^{-1}$, (b) fitting plots of MIP and NIP with the Freundlich isotherm model, and (c) binding affinity distribution for MIP and NIP within the analytical window derived from the fitting parameters of the Freundlich equation.

Table 1

Isotherm parameters for HYP on MIP and NIP estimated by fitting data to the Freundlich isotherm model.

Compound	Polymer	Relative coefficient (R^2)	m	N_{K1-K8} ($\mu\text{mol g}^{-1}$)	\bar{K}_{K1-K8} (M^{-1})
HYP	MIP	0.956	0.940	2.706	$7.95\text{E}+2$
	NIP	0.854	0.999	0.028	$3.16\text{E}+2$
Ratio MIP/NIP				96.9	2.51

assayed, the highest binding affinity is found for INO which has different shapes and greater size than the dummy template, TPH; consequently, it would experience steric exclusion in the high

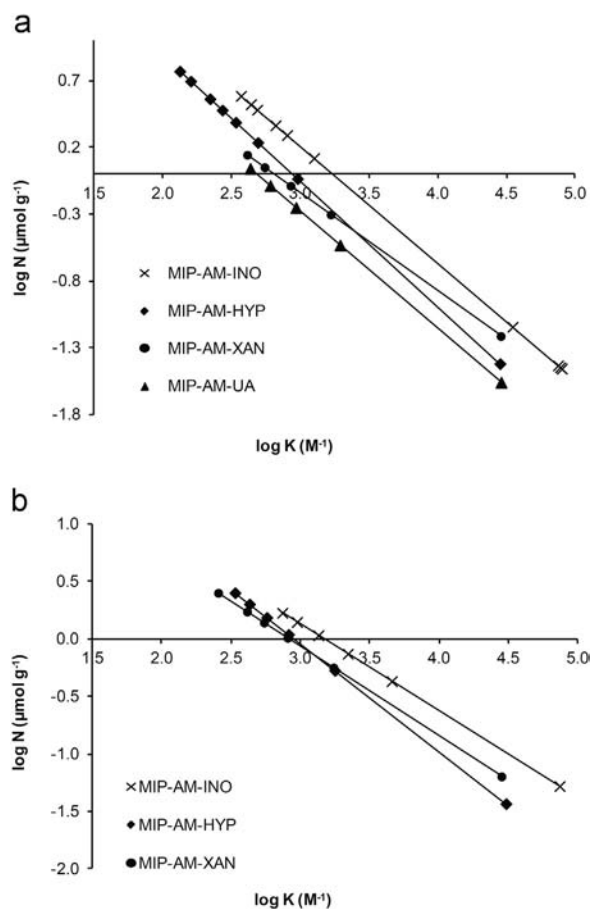


Fig. 3. (a) Individual selectivity log–log Freundlich isotherms of HYP, INO, XAN, UA on MIP and (b) cross-selectivity log–log Freundlich isotherms of HYP, INO and XAN on MIP.

Table 2

Individual selectivity parameters for INO, XAN and UA on MIP and NIP estimated by fitting data to the Freundlich isotherm model.

Compound	Polymer	Relative coefficient (R^2)	m	N_{K1-K8} ($\mu\text{mol g}^{-1}$)	\bar{K}_{K1-K8} (M^{-1})
INO	MIP	0.996	0.875	1.897	$2.50\text{E}+3$
	NIP	0.904	0.834	1.576	$6.18\text{E}+2$
Ratio MIP/NIP				1.20	4.04
XAN	MIP	0.978	0.736	0.788	$2.47\text{E}+3$
	NIP	0.805	0.884	0.545	$1.63\text{E}+3$
Ratio MIP/NIP				1.45	1.51
UA	MIP	0.825	0.877	0.531	$2.14\text{E}+3$
	NIP	0.874	0.461	1.850	$3.17\text{E}+3$
Ratio MIP/NIP				0.29	0.67

affinity binding cavities. Secondly, as stated in Section 3.1 the MIP is a non-porous matrix gel which swells in water but only a quarter the value reached in the porogen.

Conversely, as discussed by Simon et al. [54] pre-organization of functional groups may dominate the performance of MIPs designed for analytes with three or more functional groups capable of hydrogen bonding interaction with the functional monomer. Thus, the MIP may not require an exact recreation of the shape and distance parameters for binding ATP derivatives due to the presence of 2 to 4H-donor groups and 3H-acceptor groups per analyte molecule, besides abundance of low affinity binding sites within the MIP. On the other hand, the MIP-analyte interaction seems to diminish upon increasing the number of carbonyl

(C=O) groups either in the pyrimidine ring or imidazole ring of the ATP derivatives, whereas the extra three OH groups of INO may promote adsorption despite the larger size of the molecule.

3.2.2. Cross-selectivity properties

The performance of the MIP was evaluated in the presence of a mixture of INO, HYP and XAN as ATP degradation compounds to estimate its applicability in real samples. UA was not included in cross-selectivity studies due to the poor adsorption observed in individual selectivity analysis. Fig. 3(b) shows the FI in log K –log N format for cross-selectivity experiments. Apparently the plot is similar to the one described in Fig. 3(a) for individual selectivity assays: the INO line lies above the HYP and XAN lines which crossed each other. Nonetheless, the IF values differ from the individual selectivity assays. The average imprinting factor for HYP (2.06) was higher than for INO (1.32), while the IF_{max} was 5.88 and 2.37 for HYP and INO respectively. Accordingly, the average SF value for HYP related to INO was 1.56, although the SF_{max} increased up to 3.92 at the lowest concentration studied. Concerning XAN, the IF_{max} was 4.70 for the lowest concentration tested with a corresponding SF compared to HYP of 1.25, however, the IF was below 1 for higher amounts of XAN, indicating unspecific adsorption. In short, according to cross-selectivity studies, the MIP can be used as sorbent in MSPD procedure to determine HYP and INO in fish samples, since the MIP had demonstrated its efficiency to discriminate and pre-concentrate these compounds among all the ATP derivatives.

3.3. Optimization of the MIP–MSPD procedure

The influence of several parameters, such as the ratio of sample to MIP sorbent, the pH of the sorption process, the washing solvent or the elution solvent, on MIP–MSPD efficiency was investigated. A suitable sample/sorbent ratio in MSPD process could increase the interface area between the analytes and sorbent and allow complete sorption of the sample components to facilitate their transfer into sorbent. In the same way, the sequence and design of an elution profile should strive to retain the target analytes on the MIP with a high degree of specificity, while removing the sample matrix interferences as much as possible. Moreover, the MIP pre-packed in the bottom of the cartridge could act as MSPD sorbent for further removing interfering matrix components and isolate analytes to perform high recoveries [55].

3.3.1. Optimization of sample/sorbent ratio

Ratios of sample to sorbent typically range from 1:1 to 1:4, since higher or lower ratios often lead to lower recoveries because the packing material in the cartridge is more heterogeneous [56–62]. Therefore, ratios of sample/sorbent ranging from 1:1 to 1:3 were evaluated. Recoveries (R) increased from 50 to 100% upon increasing the sample: sorbent ratio from 1:1 to 1:2 ($\Delta R \sim 50\%$), then remained constant within experimental error. Accordingly, 1:2 was applied as optimum sample/sorbent ratio in the subsequent studies in order to obtain the best recoveries with the lowest polymer consumption.

3.3.2. Optimization of sorption process

pH is an important factor in the sorption process, because pH not only affects the properties of the sorbent surface, but also influences the target analyte speciation in solution and the extent of dissociation of functional groups on the active sites of the sorbent [63].

HYP is a purine with pK_a values of $pK_1 = 1.79$ – 1.90 for N_7 , $pK_2 = 8.70$ – 8.91 for the amine group close to carbonyl group and $pK_3 = 10.27$ – 12.07 for the amine group at 9 position of the purine at 25 °C (the atoms in the purines are named from 1 to 9 following conventional nomenclature rules) [64]. Under strong acidic conditions ($pH < 2$), N_7 wins one H^+ and HYP^+ becomes the main

form while at alkaline pH, HYP is present predominantly in the dissociated forms HYP^- and HYP^{2-} . The prevalence of HYP charged forms decreases the molecular recognition at the imprinting sites, reducing the sorption efficiency. Thus, the pH of the sorption step should be adjusted to neutral or slightly acidic conditions to promote extraction of neutral HYP. Moreover, these pH conditions are close to the isoelectric point (IP) of HYP ($\cong 5$) [65]; at this pH value HYP does not have any electrical charge and maximum sorption may be expected. On the other hand, only at the strongest acidic conditions ($pH < 1$), acrylamide turns into AM^+ (the carbonyl oxygen is protonated) [66] within the MIP. Under these pH conditions, HYP and AM are positively charged and electrostatic repulsive interaction between HYP and MIP occurs, leading to a decrease in molecular recognition.

To prove the influence of pH on the sorption process, HYP solutions ($182.5 \mu\text{g mL}^{-1}$) in water:ethanol (9:1) were prepared at pH values spanning from 2 to 8 by addition of hydrochloric acid or sodium hydroxide solutions; then, sorption experiments were carried out following an experimental procedure similar to batch binding. According to the preceding paragraph, quantitative sorption was obtained at $pH \geq 5$ (Fig. 4(a)). At slightly acidic and neutral conditions hydrogen bonding between the analyte and AM is maximized, whereas ionic interactions are not significant. Therefore, pH values ranging between 5 and 8 are considered the optimum pH conditions for the MSPD procedure to achieve the highest sorption capacity, conditions which are already found in fish meat.

3.3.3. Optimization of the clean-up procedure

It is generally recommended to use a solvent in the washing step as similar as possible to the nature of the sample [59]. Nonetheless, the ATP derivatives are highly water-soluble compounds and the use of the aqueous mixture, proposed as sample stimulant, probably elutes a significant portion of HYP retained in the MIP at this stage. Consequently, different washing solvents were investigated in order to remove the non-polar fraction, containing fats and other less polar compounds present in fish samples, and promote total retention of the analyte within the MIP. The solvents assayed are in increasing order of polarity: *n*-hexane, dichloromethane, the mixture *n*-hexane: dichloromethane (1:1) and acetonitrile.

No HYP was eluted when *n*-hexane was employed as washing solvent whereas the other solvents tested eluted target purines. The amount eluted increased with the solvent polarity. Different volumes of *n*-hexane, ranging from 1 to 4 mL, were further investigated. The experimental results indicated that a volume lower than 1 mL was not sufficient for purification, while 2 mL of *n*-hexane were found to be the appropriate washing volume.

3.3.4. Optimization of the elution process

The elution solvent should have enough elution ability to desorb the analyte and facilitate additional sample treatments. Initially, the optimization of the elution step was performed using a series of common elution solvents including water:AcOH (4:1), water:AcOH (9:1), water:AcOH (99:1), water:TFA (99.5:0.5) and water:TFA (99:1) respectively. Poor recoveries were obtained for HYP in all situations (2–13%), probably due to the fact that HYP remains neutral and strongly bound to AM within the MIP. It seemed clear that strong basic conditions converting HYP in the deprotonated forms are needed to remove it from the imprinted cavities. Thus, several ammonium hydroxide solutions in water at pH 9, 11 and 12.5 were evaluated as elution solvent. The solution at pH 12.5 was ammonium hydroxide (25% in water) commercial solution, while pH 11 solution (5.55 M) was prepared by dilution from the latter and pH 9 solution (5.55×10^{-6} M) was prepared by dilution from an intermediate solution of 0.01 M. The HYP elution profile was

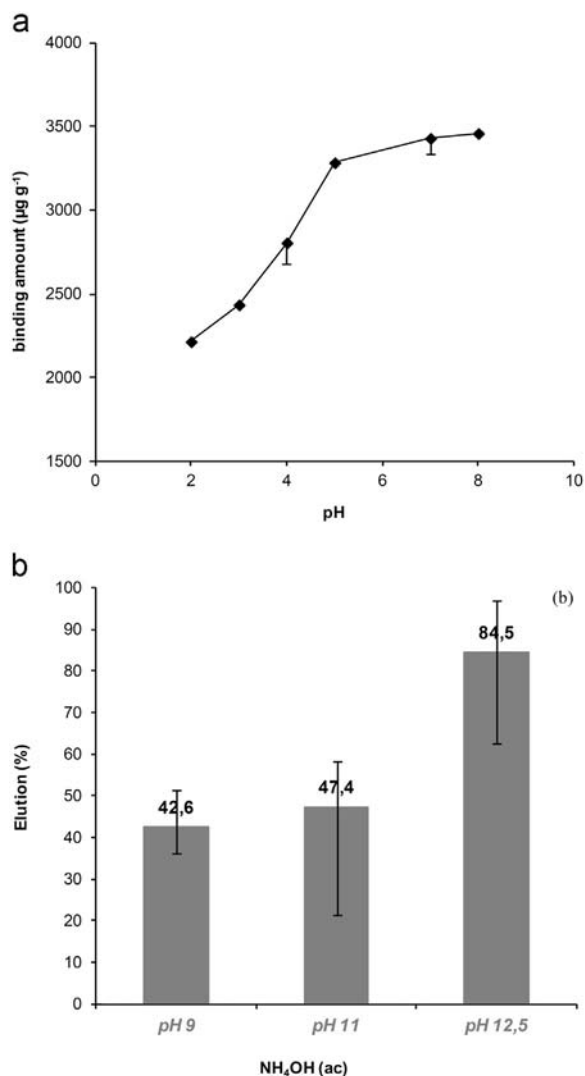


Fig. 4. (a) Sorption of HYP on MIP as function of pH (MIP dose: 0.2 g, solution volume: 4 mL, US contact time: 5 min, room temperature) and (b) influence of the elution solvents (4 mL) on the % HYP recovered.

investigated in the MIP (Fig. 4(b)). Best recoveries were obtained by using ammonium hydroxide commercial solution (pH 12.5).

Despite the fact that pH 12.5 lead to optimal elution conditions, several practical drawbacks on the application of MIP–MSPD procedure to real samples makes pH 9 the best option for final application.

From another point of view, the volume of the elution solvent loaded on the cartridge affects the recovery of HYP: small volumes lead to incomplete elution whereas excessive volumes would require a longer dryness step. After several trials, 4 mL was found to be the optimum volume. In fact, this volume of elution solvent is frequently used in MSPD procedure.

3.4. Validation of the MIP–MSPD–UPLC–PDA method

To validate the procedure, two methods of quantitative evaluation of the analysis were compared by statistical treatment and direct comparison: external calibration and standard additions [67]. External calibration curves were plotted for HYP and INO with concentration ranging from 0.05 to 25 $\mu\text{g mL}^{-1}$ and standard addition curves were plotted preparing duplicate base ‘zero’ samples and standard addition samples from 10.00 to 40.00 $\mu\text{g mL}^{-1}$. Statistical treatment applying the *t*-test for the slopes of the calibration curves has shown matrix effect for both compounds in fish samples. The use of the

Table 3
Features of the MIP–MSPD–UPLC–PDA method ($n=5$).

Analytes	Regression equation	R^2	LOD ($\mu\text{g mL}^{-1}$)	LOQ ($\mu\text{g mL}^{-1}$)	RSD (%)
HYP	$y=84.29x+6.59 \times 10^2$	0.9987	1.702	5.672	0.8
INO	$y=47.83x+4.82 \times 10^2$	0.9986	1.785	5.950	0.7

method of standard additions for the quantification of these compounds in the studied samples was thus preferred.

This MIP–MSPD–UPLC–PDA method was validated in terms of linearity, limits of detection (LOD), limits of quantification (LOQ) and precision under the selected optimum conditions. The linearity of the method was tested for HYP and INO, since selectivity experiments demonstrated that the MIP is suitable to determine both compounds. Calibration curves were constructed by performing the linear regression analysis using the chromatographic peak areas measured at three increasing spiked levels in a range of 10.00–40.00 $\mu\text{g mL}^{-1}$. This range was selected according to the ATP derivatives levels in hake samples [68,69]. The results showed good linearity for the analytes with correlation coefficients of 0.9987 for HYP and 0.9986 for INO. Detection and quantification limits were calculated according to a procedure described by Shabir [70] using the calibration graphs, being $\text{LOD}=y_B+3 \times \text{SB}$ and $\text{LOQ}=y_B+10 \times \text{SB}$. Representing y_B (blank signal)= a (intercept of the calibration graph) and SB (standard deviation of the blank)= S_y/x . Relative standard deviations (RSDs) were evaluated by performing replicate analysis of the middle spiked level (20 $\mu\text{g mL}^{-1}$) (Table 3).

Precision was calculated in terms of intra-day repeatability and inter-day reproducibility. The intra-day repeatability was performed by analyzing spiked fish samples five times in one day at three different fortified concentrations (10.00, 20.00 and 40.00 $\mu\text{g mL}^{-1}$) for HYP and INO. RSDs values lied between 0.84% and 7.50% for HYP and between 1.05% and 13.0% for INO. The inter-day reproducibility was performed similarly over three consecutive days and RSDs were in the range of 2.84–8.91% for HYP and 2.68–13.6 for INO.

3.5. Analysis of fish samples

To evaluate the performance of the proposed MIP–MSPD–UPLC–PDA method, three commercial defrosted hake samples were pretreated under MIP–MSPD procedure. The results which are shown in Table 4 lie well above the quantification limit except for sample 1. Besides, INO values were greater than those of HYP, according to the trend shown by most fish species studied in subsequent days after the capture [68,69].

Moreover, a recovery study was carried out to develop a more detailed analysis of the sample matrix effect by spiking three different levels of HYP and INO into the hake samples (10.00–40.00 $\mu\text{g mL}^{-1}$). High recoveries were obtained after MIP–MSPD pre-treatment. Recoveries ranged from 103.1% to 113.4% with an average RSD $\leq 4.2\%$ in all cases (Table 5).

As a final point, endogenous interferences from the fish muscle were eluted out in the washing fraction so that clean chromatograms of both original and spiked samples were obtained at the end of the process, demonstrating the excellent purification ability and high affinity and selectivity of the MIP–MSPD protocol for HYP and INO; hence, it can be potentially applied for the determination of these compounds in complicated bio-matrix samples (Fig. 5).

4. Conclusion

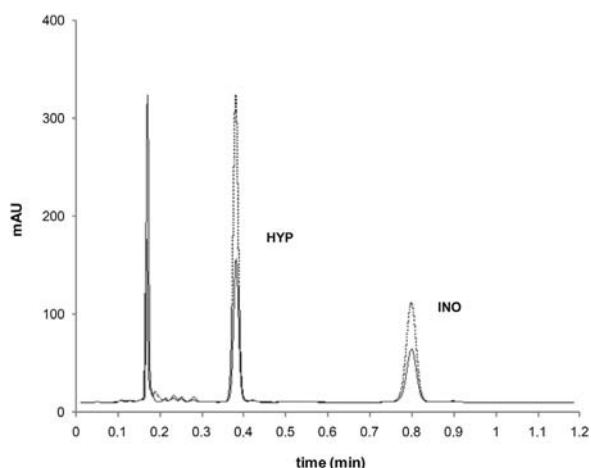
A novel, simple and reliable MIP–MSPD–UPLC–PDA method was developed for selective extraction and purification of HYP and

Table 4Contents of the nucleotides in hake samples ($n=3$).

Hake sample	HYP ($\mu\text{g mL}^{-1}$)	INO ($\mu\text{g mL}^{-1}$)
1	D ^a	D ^a
2	12.55	13.34
3	7.821	10.08

^a Detectable but not quantifiable.**Table 5**Recoveries of the MIP–MSPD–UPLC–PDA method for spiked hake samples ($n=3$).

Spiked level of the analytes	10.00 $\mu\text{g mL}^{-1}$		20.00 $\mu\text{g mL}^{-1}$		40.00 $\mu\text{g mL}^{-1}$	
	Recovery (%)	RSD (%)	Recovery (%)	RSD (%)	Recovery (%)	RSD (%)
HYP	113.4	4.0	110.9	2.2	106.5	1.5
INO	111.2	4.2	108.2	1.7	103.1	2.1

**Fig. 5.** Chromatograms of the hake samples (— hake sample — spiked hake sample) after the MIP–MSPD protocol.

INO ATP derivatives used as freshness index in fish samples. The method is based on the selective retention of HYP and INO (at pH near IP in neutral forms) in a polar sorbent (MIP), elimination of less polar interferences with *n*-hexane and selective elution of the analytes with NH_4OH aqueous solution at pH 9 (anionic forms). The method has been validated by analyzing three commercial defrosted hake samples at spiked levels of 10.00–40.00 $\mu\text{g mL}^{-1}$. All recoveries were around 100% and RSD of repeatability and reproducibility were $\leq 4.2\%$.

The developed method combines the high affinity and selectivity of MIP technology with the simple, rapid and efficient sample pre-treatment of MSPD plus the highly effective separation of UPLC, to achieve a significant time reduction of the total analytical process. In addition to the analytical advantages, the method has other practical improvements over conventional methods of sample treatment, such as lower cost, lower consumption of organic solvents and simple instrumentation involved.

Acknowledgments

The study was financially supported by the Ministerio de Ciencia e Innovación and FEDER (Ref. no.: IPT-060000-2010-14 MIPFOOD, 6PN Subprograma INNFACTO).

References

- L. Mora, A.S. Hernández-Cázares, M.C. Aristoy, F. Toldrá, *Food Chem.* 123 (2010) 1282–1288.
- N. Batlle, M.C. Aristoy, F. Toldrá, *J. Food Sci.* 65 (3) (2000) 413–416.
- R. Tsai, R.G. Cassens, E.J. Briskey, M.L. Greaser, *J. Food Sci.* 37 (1972) 612–616.
- M.E. Surette, T.A. Gill, P.J. LeBlanc, *J. Agric. Food Chem.* 36 (1988) 19–22.
- V. Venugopal, *Biosens. Bioelectron.* 17 (2002) 147–157.
- A. Mulchandani, J.H.T. Luong, K.B. Male, *Anal. Chim. Acta* 221 (1989) 215–222.
- M.T. Veciana-Nogues, M. Izquierdo-Pulido, M.C. Vidal-Carou, *Food Chem.* 59 (1997) 467–472.
- L. Gil, J.M. Barat, E. Garcia-Breijo, J. Ibañez, R. Martínez-Mañez, J. Soto, E. Llobet, J. Brezmes, M.C. Aristoy, F. Toldrá, *Sens. Actuators B* 131 (2008) 362–370.
- G. Volpe, M. Mascini, *Talanta* 43 (1996) 283–289.
- D. Balladín, D. Narinesingh, V. Stoute, T. Ngo, *Appl. Biochem. Biotechnol.* 62 (1997) 317–328.
- E. Watanabe, K. Ando, I. Karube, H. Matsuoka, S. Suzuki, *J. Food Sci.* 48 (1983) 496–500.
- M.A. Carsol, G. Volpe, M. Mascini, *Talanta* 44 (1997) 2151–2159.
- Y. Yano, N. Miyaguchi, M. Watanabe, T. Nakamura, T. Youdou, J. Miyai, M. Numatab, Y. Asano, *Food Res. Int.* 28 (1995) 611–617.
- Y. Yano, N. Kataho, M. Watanabe, T. Nakamura, Y. Asano, *Food Chem.* 52 (1995) 439–445.
- A.T. Lawal, S.B. Adeloju, *Talanta* 100 (2012) 217–228.
- R. Grau, A.J. Sánchez, J. Girón, E. Iborra, A. Fuentes, J.M. Barat, *Food Res. Int.* 44 (2011) 331–337.
- A.S. Hernández-Cázares, M.C. Aristoy, F. Toldrá, *Food Chem.* 123 (2010) 949–954.
- N. Batlle, M.C. Aristoy, F. Toldrá, *J. Food Sci.* 66 (2001) 68–71.
- T.L. Scheffler, D.E. Gerrard, *Meat Sci.* 77 (2007) 7–16.
- T. Richter, L.L. Shultz-Lockyear, R.D. Oleschuk, U. Bilitewski, D.J. Harrison, *Sens. Actuators B* 81 (2002) 369–376.
- A.L. Nguyen, J.H.T. Luong, C. Masson, *Anal. Chem.* 62 (1990) 2490–2493.
- B. Roberts, B.A. Morris, M.N. Clifford, *Food Chem.* 42 (1991) 1–17.
- G. Van den Thillart, A. Van Waarde, H.J. Muller, C. Erkelens, J. Lugtenburg, *Comp. Biochem. Physiol.* 95B (1990) 789–795.
- J. Pei, X.Y. Li, *Anal. Chim. Acta* 414 (2000) 205–213.
- Y. Lui, N. Lo, W. Tao, S. Yao, *Electroanalysis* 16 (2004) 1271–1278.
- H.S. Nakatani, L.V. Santos, C.P. Pelegrine, M. Gomes, M. Matsushita, N.E. Desouza, J.V. Visentainer, *Am. J. Biochem. Biotechnol.* 1 (2005) 85–89.
- N. Cooper, R. Khosravan, C. Erdmann, J. Fiene, J.W. Lee, *J. Chromatogr. B* 837 (2006) 1–10.
- M.L. Dornelles, K.L. Tatsuo, *Food Chem.* 77 (2002) 237–256.
- A. Martín-Esteban, *Trends Anal. Chem.* 45 (2013) 169–181.
- E. Caro, R.M. Marcé, F. Borrull, P.A.G. Cormack, D.C. Sherrington, *Trends Anal. Chem.* 25 (2006) 143–154.
- N. Fontanals, R.M. Marcé, F. Borrull, *J. Chromatogr. A* 1152 (2007) 14–31.
- F.G. Tamayo, E. Turiel, A. Martín-Esteban, *J. Chromatogr. A* 1152 (2007) 32–40.
- S.A. Barker, *J. Biochem. Biophys. Methods* 70 (2007) 151–162.
- E.M. Kristenson, L. Ramos, U.A.Th. Brinkman, *Trends Anal. Chem.* 25 (2006) 96–111.
- S.A. Barker, *J. Chromatogr. A* 880 (2000) 63–68.
- S.A. Barker, *J. Chromatogr. A* 885 (2000) 115–127.
- N.R. Jones, J. Murray, *J. Sci. Food Agric.* 13 (1962) 475–480.
- M. Tikik, K. Tikik, M.A. Torngren, L. Meiner, M.D. Aaslyng, A.H. Karlsson, *J. Agric. Food Chem.* 54 (2006) 7769–7777.
- D. Farthing, D. Sica, T. Gehr, B. Wilson, I. Fakhry, T. Larus, C. Farthing, H.T. Karnes, *J. Chromatogr. B* 854 (2007) 158–164.
- A. Lasagabaster-Latorre, M.C. Cela-Pérez, S. Fernández-Fernández, J.M. López-Vilariño, M.V. González Rodríguez, Selective removal of ATP degradation products from food matrices I: design and characterization of a dummy molecularly imprinted specific sorbent for hypoxanthine (unpublished Results).
- Commission Regulation (EU) No. 10/2011 of 14 January 2011 on plastic materials and articles intended to come into contact with food Text with EEA relevance, *Official Journal of European Communities*, 2011, L 12, 1.
- D.A. Spivak, *Adv. Drug Deliv. Rev.* 57 (2005) 1779–1794.
- M. Castro López, M.C. Cela Pérez, M.S. Dopico García, J.M. López Vilariño, M.V. González Rodríguez, L.F. Barral Losada, *Anal. Chim. Acta* 721 (2012) 68–78.
- M.C. Cela-Pérez, M.M. Castro-López, A. Lasagabaster-Latorre, J.M. López-Vilariño, M.V. González-Rodríguez, L.F. Barral-Losada, *Anal. Chim. Acta* 706 (2011) 275–284.
- B. Sellergrén, K.J. Shea, *J. Chromatogr.* 635 (1993) 31–49.
- S.V. Duy, I. Lefebvre-Tournier, V. Pichon, F. Hugon-Chapuis, J. Puy, C. Périgaud, *J. Chromatogr. B* 877 (2009) 1101–1108.
- N.S. Bibi, L. Galvis, M. Grasselli, M. Fernández-Lahore, *Process Biochem.* 47 (2012) 1327–1334.
- Y. Hu, Y. Li, R. Liu, W. Tan, G. Li, *Talanta* 84 (2011) 462–470.
- B. Sellergrén, *Trends in Anal. Chem.* 18 (3) (1999) 164–174.
- N.W. Turner, E.V. Piletska, K. Karim, M. Whitcombe, M. Malecha, N. Magan, C. Baggiani, S.A. Piletsky, *Biosens. Bioelectron.* 20 (2004) 1060–1067.
- H. Zhang, *Polymer* 55 (2014) 699–714.
- Y. Zhang, Y. Li, Y. Hu, G. Li, Y. Chen, *J. Chromatogr. A* 1217 (2010) 7337–7344.

- [53] N. Henry, R. Delepee, J.M. Seigneuret, L.A. Agrofoglio, *Talanta* 99 (2012) 816–823.
- [54] R. Simon, M.E. Collins, D.A. Spivak, *Anal. Chim. Acta* 591 (2007) 7–16.
- [55] H. Yan, H. Wang, J. Qiao, G. Yang, *J. Chromatogr. A* 1218 (2011) 2182–2188.
- [56] F. Qiao, H. Yan, *J. Chromatogr. B* 879 (2011) 3551–3555.
- [57] F. Qiao, H. Sun, *J. Pharm. Biomed.* 53 (2010) 795–798.
- [58] F. Quiao, J. Du, *J. Chromatogr. B* 923–924 (2013) 136–140.
- [59] H. Sun, F. Qiao, G. Liu, S. Liang, *Anal. Chim. Acta* 625 (2008) 154–159.
- [60] L. Enríquez-Gabeiras, A. Gallego, R.M. Garcinuño, P. Fernández-Hernando, J.S. Durand, *Food Chem.* 135 (2012) 193–198.
- [61] H. Yan, F. Wang, H. Wang, G. Yang, *J. Chromatogr. A* 1256 (2012) 1–8.
- [62] H. Yan, X. Cheng, N. Sun, T. Cai, R. Wu, K. Han, *J. Chromatogr. B* 908 (2012) 137–142.
- [63] C.M. Dai, J. Zhang, Y.L. Zhang, X.F. Zhou, Y.P. Duan, S.G. Liu, *Chem. Eng. J.* 211–212 (2012) 302–309.
- [64] J.J. Christensen, J.H. Rytting, R.M. Izzat, *Biochemistry* 9 (1970) 4907–4913.
- [65] M. Soleimani, S. Ghaderi, M.G. Afshar, S. Soleimani, *Microchem. J.* 100 (2012) 1–7.
- [66] Marvin was used for drawing, displaying and characterization chemical structures, substructures and reactions, Marvin 14.12.8.0, 2014, ChemAxon (<http://www.chemaxon.com>).
- [67] M.M. Castro-López, J.M. López-Vilariño, M.V. González-Rodríguez, L.F. Barral-Losada, *Microchem. J.* 99 (2011) 461–469.
- [68] J.M. Barat, L. Gil, E. Garcia-Breijo, M.C. Aristoy, F. Toldrá, R. Martínez-Máñez, J. Soto, *Food Chem.* 108 (2008) 681–688.
- [69] P.T. Lakshmanan, P.D. Antony, K. Gopakumar, *Food Control* 7 (1996) 277–283.
- [70] G.A. Shabir, *J. Chromatogr. A* 987 (2003) 57–66.